Chemosphere 192 (2018) 171–177

Contents lists available at ScienceDirect

Chemosphere

journal homepage: www.elsevier.com/locate/chemosphere

In vitro assessment of the toxicity of lead (Pb^{2+}) to phycocyanin

Songwen Tan [a], Xu Tan [b], Zhenxing Chi [a, c, d, *], Dayin Zhang [a], Weiguo Li [a]

[a] Department of Environmental Engineering, Harbin Institute of Technology, Weihai, 2# Wenhua West Road, Weihai 264209, PR China
[b] Department of Civil and Environmental Engineering, University of Technology Sydney, Sydney 2007, Australia
[c] State Key Laboratory of Urban Water Resource and Environment, Harbin Institute of Technology, 73# Huanghe Road, Harbin 150090, PR China
[d] Guangzhou Key Laboratory of Environmental Exposure and Health, School of Environment, Jinan University, Guangzhou 510632, PR China

HIGHLIGHTS

- Toxicity of Pb^{2+} to phycocyanin is assessed *in vitro*.
- Fluorescence quenching process of phycocyanin by Pb^{2+} is static.
- Pb^{2+} affect the Tyr residues more than the Trp residues.
- Pb^{2+} affect the phycocyanin skeleton and its secondary structure.

GRAPHICAL ABSTRACT

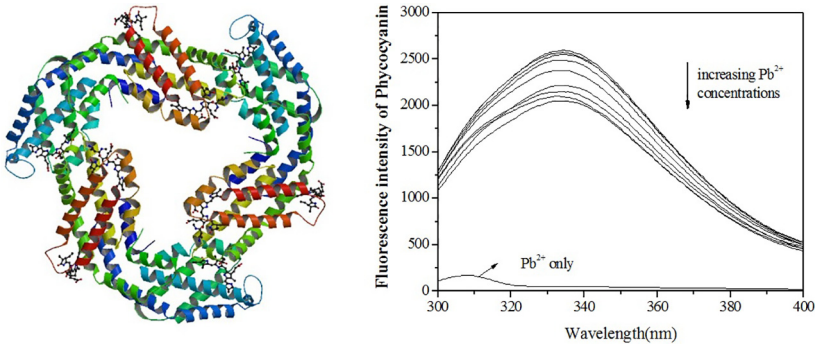

ARTICLE INFO

Article history:
Received 30 August 2017
Received in revised form
22 October 2017
Accepted 28 October 2017
Available online 28 October 2017

Handling Editor: Frederic Leusch

Keywords:
Lead
Phycocyanin
Toxicity
Fluorescence characteristics
Protein structure

ABSTRACT

This work reports the influence of lead (Pb^{2+}) on fluorescence characteristics and protein structure of phycocyanin molecules experimentally *in vitro*. The fluorescence intensity decreases with the increasing concentration of Pb^{2+} from 0 to 5×10^{-5} mol L^{-1}, showing the fluorescence quenching of phycocyanin by Pb^{2+}. The quenching process is suggested to be static regarding the calculation results and the experimental results of time-resolved fluorescence decay profiles. The synchronous fluorescence spectra show that the effect of Pb^{2+} on the Tyr residues of phycocyanin is more significant than the Trp residues. The forming of aggregation by the interaction of Pb^{2+} with phycocyanin molecules is suggested from the results of resonance light scattering spectra. The UV–Vis spectra of the protein skeleton of phycocyanin have a red-shift of about 10 nm with increasing the Pb^{2+} concentration from 0 to 5×10^{-5} mol L^{-1}, indicating a change in the protein skeleton and its secondary structure. With the increasing Pb^{2+} concentration, the two negative peaks (209 nm and 218 nm) on circular dichroism spectra become smaller, showing a decrease of the α-helix structure. These results may give people a deeper understanding of that how the heavy metal (Pb^{2+}) can affect the chemo-physical properties of phycocyanin.

1. Introduction

During the past decades, lead (Pb^{2+}) is recognized as one of the main environmental pollutants from industry (Zhang et al., 2012; More et al., 2017). As a result of river inputs the oceans have been

* Corresponding author. Department of Environmental Engineering, Harbin Institute of Technology, Weihai, 2# Wenhua West Road, Weihai 264209, PR China.
E-mail address: zhenxingchi@gmail.com (Z. Chi).

https://doi.org/10.1016/j.chemosphere.2017.10.159
0045-6535/

polluted for years, and the bioaccumulation and chelation of lead by marine organisms keep the concentration of lead at high pollution levels (do Sul and Costa, 2014; Burnett and Patterson, 2015; Raspor et al., 2015). There have been many works in toxicology, marine biology and ecology reported on the toxicity of lead to the marine organisms, regarding DNA damage, enzyme inhibition, and so forth (Tao et al., 2000; Tang et al., 2013; Peng et al., 2015).

In the marine ecosystem, cyanobacteria is an important phylum of microorganism that has phycocyanin protein in their living cells. Phycocyanin is a natural protein with red fluorescence from cyanobacteria for the photosynthetic apparatus, converting the solar energy into their chemical energy (Patel et al., 2005). The phycocyanin contains phycocyanobilins (linear tetrapyrrole molecules with florescent property) and cysteine amino acid residues (Kannaujiya et al., 2016). The energy transitions of pi-pi* within the florescent molecules are related with the photoluminescence characteristics (Stoll et al., 2009). Since the interactions of heavy metal ions with phycocyanin protein lead to the fluorescence quenching of phycocyanin (Saha et al., 2011; Bhayani et al., 2016), the phycocyanin fluorescence in the cyanobacterial cells can be used as bioindicator for monitoring heavy metals in drinking water regarding the high sensitivity and responding speed (Jusoh et al., 2017).

Some studies of cyanobacteria have reported the toxicity of Pb^{2+} on phycocyanin. For *Synechocystis* sp. (Arunakumara and Zhang, 2009), the phycocyanin content decreased with increasing Pb^{2+} concentration. 29.34% inhibition of phycocyanin were observed when the *Synechocystis* sp. cells exposed to 6 mg/L Pb^{2+}. Their result agreed with the report by Gelagutashvili (2007) that the fluorescence of phycocyanin decreased with increasing Pb^{2+} concentration, due to high affinity of phycocyanin-Pb^{2+} resulting in fluorescence quenching. However in another work, 5 mg/L Pb^{2+} stimulated the growth of cells of *Spirulina* sp. while no much influence was observed on the pigment contents at this low concentration of Pb^{2+} (Arunakumara et al., 2008). Yet no specific research has focused on the toxicity of Pb^{2+} to phycocyanin at molecular level experimentally. In this work, an overall study is carried out to assess the influence of Pb^{2+} on fluorescence characteristics and protein structure of phycocyanin molecules *in vitro*. The results may give people a deeper understanding of that how the heavy metal (Pb^{2+}) can affect the chemo-physical properties of phycocyanin.

2. Materials and methods

2.1. Materials

The phycocyanin, isolated from *Spirulina platensis* (*Arthrospira platensis*), has a molecular weight of ~120,000 Da at pH of 6.5–8.0 and was purchased from Zhejiang Binmei Biotechnology Co. Ltd., China. Monosodium orthophosphate ($NaH_2PO_4…2H_2O$) and disodium hydrogen phosphate ($Na_2HPO_4…12H_2O$) were obtained from Sinopharm Chemical Reagent Co. Ltd. And were used to prepare the phosphate buffer saline (pH = 7.0). Lead (II) nitrate ($Pb(NO_3)_2$) was obtained from Sigma-Aldrich, China. All chemicals were analytical reagent grade.

2.2. Fluorescence characteristics

Phycocyanin samples with volume of 10 mL were prepared by mixing the phosphate buffer saline, phycocyanin and $Pb(NO_3)_2$ solution for 25 min. The fluorescence spectra of the phycocyanin samples with Pb^{2+} concentrations of ($x10^{-6}$ mol L^{-1}) 0, 0.5, 1, 2.5, 5, 7.5, 10, 17.5, 25, 45 and 50 were measured at 298 K and 308 K. The concentration of phycocyanin samples was 5.0×10^{-7} mol L^{-1} and the pH of solutions was 7.0. The samples were placed in the F4600 Fluorescence Spectrometer (Hitachi, Japan) for analysis. The excitation wavelength was set at 278 nm with emission wavelength range set at 280–530 nm. The slit width was 5 nm and the voltage was 400 V. The results were plotted using the Stern-Volmer equation ($F_0/F = 1 + K_{SV}[Q]$) for dynamic quenching (Geethanjali et al., 2015) and modified Lineweaver-Burk equation ($\lg(F_0-F)/F = \lg K + n\lg[Q]$) for static quenching (Fu et al., 2016) to calculate the values of K_{SV}, K and n. In the equations, F_0 and F are the fluorescence intensities in the absence and presence of Pb^{2+}; K_{SV} is the quenching constants; Q is the concentration of Pb^{2+}; K is the binding constant; n is the number of binding site. The time-resolved fluorescence decay profiles were measured for the phycocyanin samples with the Pb^{2+} concentrations of ($x10^{-6}$ mol L^{-1}) 0, 6, 9 and 50 to further confirm whether the fluorescence quenching is dynamic or static (Gu et al., 2017).

The synchronous fluorescence spectra of phycocyanin samples with the Pb^{2+} concentrations of ($x10^{-6}$ mol L^{-1}) 0, 0.5, 1, 2.5, 5, 7.5, 10, 17.5, 25 and 50 were measured at $\Delta\lambda$ of 60 nm (for Tyr emission spectra) or 15 nm (for Trp emission spectra) (Bobone et al., 2014). The concentration of phycocyanin was 5.0×10^{-7} mol L^{-1}. The temperature was 298 K. The pH was 7.0. The excitation wavelength was set at 278 nm with emission wavelength range set at 280–530 nm. The slit width was 5 nm and the voltage was 400 V. The F_0/F values were plotted with the Pb^{2+} concentrations for the synchronous fluorescence spectra of phycocyanin samples at $\Delta\lambda$ of 60 nm or 15 nm.

The resonance light scattering (RLS) spectra of phycocyanin-Pb^{2+} solution, phycocyanin solution, Pb^{2+} solution and pure water were measured at 298 K to identify if the solutes were well-mixed in solution (Pasternack and Collings, 1995). The concentration of phycocyanin and Pb^{2+} were 5.0×10^{-7} mol L^{-1} and 5.0×10^{-6} mol L^{-1}, respectively. The pH is 7.0. The excitation wavelength was set at 228 nm with emission wavelength range set at 220–800 nm. The slit width was 2.5 nm and the voltage was 400 V.

2.3. Effect on the molecular structure of phycocyanin protein

The phycocyanin samples with volume of 10 mL were prepared by mixing the phosphate buffer saline, phycocyanin and $Pb(NO_3)_2$ solution for 25 min. The UV–Vis spectra of phycocyanin samples with the Pb^{2+} concentrations of ($x10^{-6}$ mol L^{-1}) 0, 0.5, 1, 2.5, 5, 7.5, 10, 17.5, 25 and 50 were measured using the UV–Vis spectrophotometer (Shimadzu UV-2450, Japan). The temperature was 298 K. The concentration of phycocyanin samples was 5.0×10^{-7} mol L^{-1} and the pH of solutions was 7.0. The scan range was set at 190–800 nm to study the effect of Pb^{2+} on protein structure of phycocyanin, including protein skeleton (200–250 nm), Phe residue (260–300 nm), disulfide bond (300–450 nm) and tetrapyrrole (550–650 nm). The slit width was 1 nm.

The circular dichroism (CD) spectra of phycocyanin samples with the Pb^{2+} concentrations of ($x10^{-6}$ mol L^{-1}) 0, 1, 2.5, 5 and 10 were measured using the CD Spectrometer (Jasco J-810, Japan). The scan range was set at 190–260 nm to study the change in α-helix structure (204–228 nm) of the phycocyanin protein.

3. Results and discussion

3.1. The interaction mechanism of Pb^{2+} with phycocyanin

The binding interaction of Pb^{2+} with phycocyanin is investigated by fluorescence, time-resolved fluorescence, synchronous fluorescence, and RLS techniques.

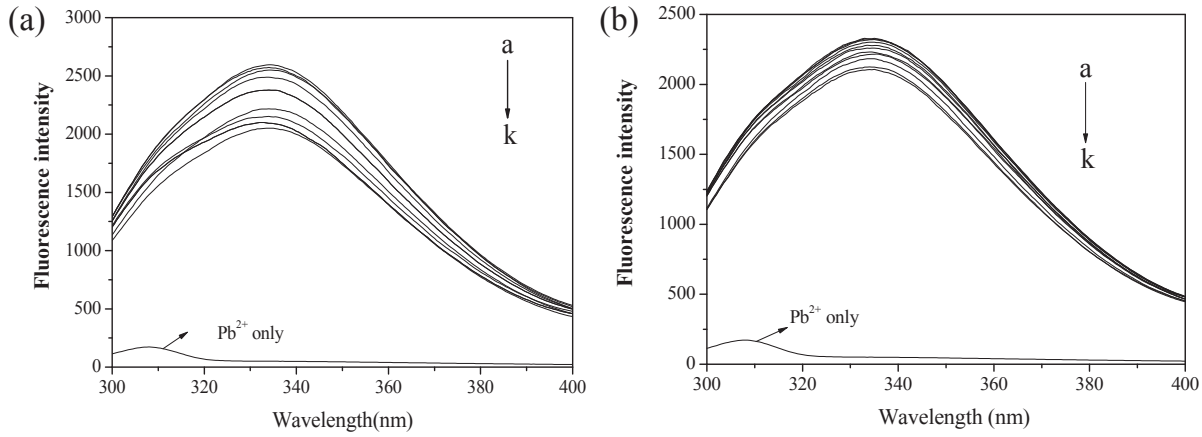

Fig. 1. Fluorescence spectra of the phycocyanin samples with Pb^{2+} concentrations of ($x10^{-6}$ mol L^{-1}) 0, 0.5, 1, 2.5, 5, 7.5, 10, 17.5, 25, 45 and 50 (from sub-a to sub-k) at 298 K (a) and 308 K (b); Concentration of phycocyanin is 5.0×10^{-7} mol L^{-1}; pH is 7.0.

Fig. 1 show the fluorescence spectra of phycocyanin samples with Pb^{2+} concentrations of ($x10^{-6}$ mol L^{-1}) 0, 0.5, 1, 2.5, 5, 7.5, 10, 17.5, 25, 45 and 50 at 298 K (Fig. 1a) and 308 K (Fig. 1b). Overall, the peaks of these fluorescence spectra locate at 335 nm. The adding of Pb^{2+} does not shift the peaks significantly. However, the fluorescence intensity decreases with the increasing concentration of Pb^{2+} from 0 to 5×10^{-5} mol L^{-1}, showing the fluorescence quenching of phycocyanin by Pb^{2+}. At 298 K the fluorescence intensity of phycocyanin decreased from about 2600 to 2100 ($\Delta = -500$), while at 308 K the fluorescence intensity decreased from about 2300 to 2100 ($\Delta = -200$), suggesting a static quenching phenomenon for the following reasons (Gu et al., 2017). Static quenching happens when the quencher binds with the fluorophore, where high temperature limits the binding force and quenching degree. Dynamic quenching happens when the quencher and fluorophore collide, where high temperature provides more energy for the collision resulting in more loss of fluorescence intensity. In addition, when the concentration of Pb^{2+} is lower than 1×10^{-5} mol L^{-1}, the K_{sv} values of Stern-Volmer equation (Fig. 2a) for dynamic quenching are calculated to be 15.6×10^3 $mol^{-1}L$ (collisional quenching constant: 15.6×10^{11} $mol^{-1}s^{-1}L$) at 298 K and 4.32×10^3 $mol^{-1}L$ (collisional quenching constant: 4.32×10^{11} $mol^{-1}s^{-1}L$) at 308 K. When the concentration of Pb^{2+} is higher than 1×10^{-5} mol L^{-1}, the K_{sv} values are calculated to be 2.14×10^3 $mol^{-1}L$ (collisional quenching constant: 2.14×10^{11} $mol^{-1}s^{-1}L$) at 298 K and 1.52×10^3 $mol^{-1}L$ (collisional quenching constant: 1.52×10^{11} $mol^{-1}s^{-1}L$) at 308 K. However, these collisional quenching constants are much larger than the maximum collision quenching constant which is 0.2×10^{11} $mol^{-1}s^{-1}L$ for biomolecules (Rasoulzadeh et al., 2010), suggesting that the Pb^{2+} quenching process is not dynamic. Calculated by the modified Lineweaver-Burk equation (Fig. 2b) for static quenching, the n values are 1.05 (at 298 K) and 1.01 (at 308 K) when the concentration of Pb^{2+} is lower than 1×10^{-5} mol L^{-1}, while the n values are 0.28 (at 298 K) and 0.55 (at 308 K) when the concentration of Pb^{2+} is higher than 1×10^{-5} mol L^{-1}. For a static quenching process, the lifetime of excited fluorophore was not affected by the quencher (Chi et al., 2016, 2017). Fig. 3 show the time-resolved fluorescence decay profiles of phycocyanin samples with different Pb^{2+} concentration. The lifetimes of phycocyanin samples were 3.39 ns, 3.41 ns, 3.43 ns and 3.39 ns, respectively, when the Pb^{2+} concentrations were ($x10^{-6}$ mol L^{-1}) 0, 6, 9 and 50. These similar values of the fluorescence lifetimes agree with that the Pb^{2+} quenching process is static. The binding of Pb^{2+} to phycocyanin may involve four kinds of forces, namely hydrogen bonding, van der Waals (VDW) interactions, hydrophobic force and electrostatic force. The relationship between molecular interactions and thermodynamic parameters has been reported in literature (Ross and Subramanian, 1981; Aki and Yamamoto, 1989): When ΔS and ΔH are negative there are hydrogen bonding and VDW interactions between

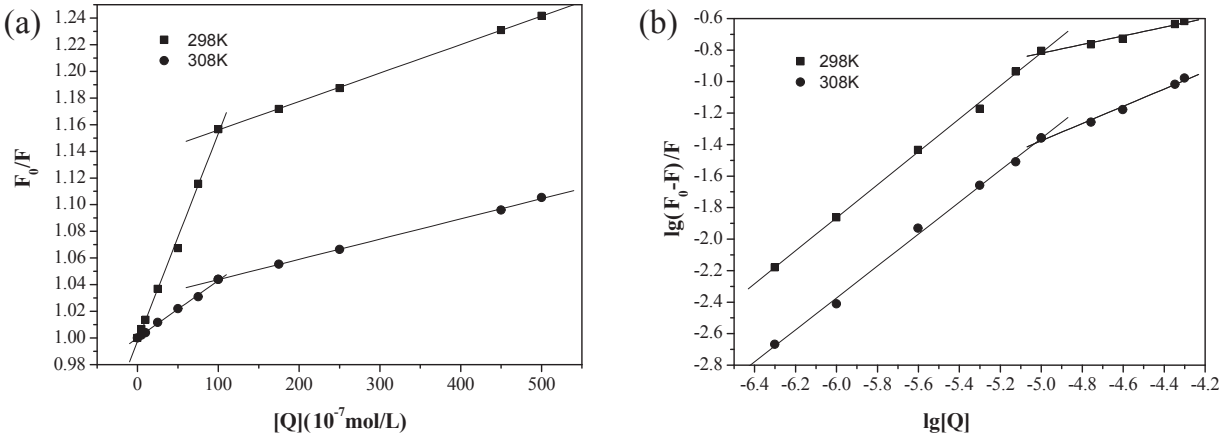

Fig. 2. The Stern-Volmer plot (a) and the Lineweaver-Burk log-log plot (b) of fluorescence quenching by Pb^{2+} for phycocyanin samples at 298 K and 308 K; Concentration of phycocyanin is 5.0×10^{-7} mol L^{-1}; pH is 7.0.

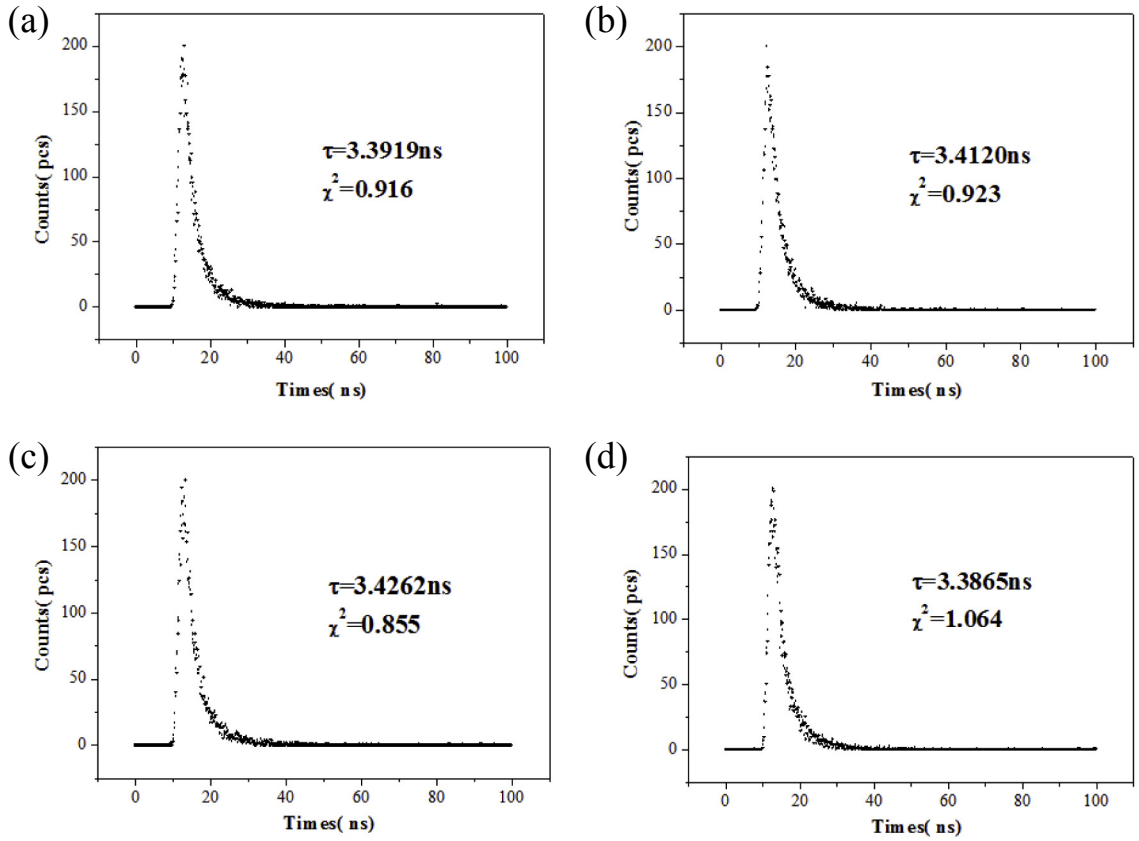

Fig. 3. Time-resolved fluorescence decay profiles of phycocyanin samples with the Pb^{2+} concentrations of ($x10^{-6}$ mol L^{-1}) 0 (a), 6 (b), 9 (c) and 50 (d) at 298 K; Concentration of phycocyanin is 5.0×10^{-7} mol L^{-1}; pH is 7.0.

molecules; When ΔS and ΔH are positive there is hydrophobic force between molecules; When ΔS is positive but ΔH is negative there is electrostatic force. Table 1 listed the thermodynamic parameters for the phycocyanin-Pb^{2+} interactions with different Pb^{2+} concentration at 298 K and 308 K. Overall, the ΔG values are negative showing that the quenching process is spontaneous. When the concentration of Pb^{2+} is lower than 1×10^{-5} mol L^{-1}, there are hydrogen bonding and VDW interactions between Pb^{2+} and phycocyanin molecules at 298 K or 308 K (ΔH<0, ΔS<0, ΔG<0). When the concentration of Pb^{2+} is higher than 1×10^{-5} mol L^{-1}, there is hydrophobic force between Pb^{2+} and phycocyanin molecules (ΔH>0, ΔS>0, ΔG<0).

The synchronous fluorescence spectra are used to study the change in amino acid residues of phycocyanin molecules. Fig. 4a shows the synchronous fluorescence spectra of phycocyanin samples for Trp emission spectra at Δλ of 60 nm. With increasing the concentration of Pb^{2+}, the fluorescence intensity of phycocyanin decreases from 2700 to 2500 (Δ = −200) and the F_0/F value decreases from 1.00 to 0.93 (Δ = −0.07, Fig. 4b). Fig. 4c shows the synchronous fluorescence spectra of phycocyanin samples for Tyr emission spectra at Δλ of 15 nm. With the increasing Pb^{2+} concentration, the fluorescence intensity of phycocyanin largely decreases from 1400 to 900 (Δ = −500) and the F_0/F value decreases from 1.00 to 0.67 (Δ = −0.33, Fig. 4d). Therefore the effect of Pb^{2+} on the Tyr residues of phycocyanin is more significant than the Trp residues.

Fig. 5 shows the RLS spectra of phycocyanin-Pb^{2+} solution, phycocyanin solution, Pb^{2+} solution and pure water. If the RLS intensity of mixture would be larger than the sum of the intensities of each solution, otherwise there would be aggregation of molecules (Pasternack and Collings, 1995). From Fig. 5, it can be seen that the RLS intensity (670) of phycocyanin-Pb^{2+} solution is larger than the sum (580) of the intensities of each solution, meaning that the interaction of Pb^{2+} and phycocyanin molecules can form aggregation.

Table 1
Thermodynamic parameters for the phycocyanin-Pb^{2+} interactions.

	T(K)	ΔH(KJ·mol^{-1})	ΔS(J·mol^{-1}K^{-1})	ΔG(KJ·mol^{-1})
C(Pb^{2+})≤1 × 10^{-5}	298	−124.55	−333.440	−25.19
mol L^{-1}	308			−21.85
C(Pb^{2+})≥1 × 10^{-5}	298	140.61	482.52	−3.18
mol L^{-1}	308			−8.01

3.2. Change in the molecular structure of phycocyanin protein

Fig. 6a shows the UV–Vis spectra of phycocyanin samples with the Pb^{2+} concentrations of ($x10^{-6}$ mol L^{-1}) 0, 0.5, 1, 2.5, 5, 7.5, 10, 17.5, 25 and 50. The UV–Vis spectra have four main peaks, locating in the range of 200–250 nm for protein skeleton, 260–300 nm for Phe residue, 300–450 nm for disulfide bond and 550–650 nm for tetrapyrrole. Fig. 6b shows the UV–Vis spectra of the protein skeleton of phycocyanin that the spectra have a red-shift of about 10 nm with increasing the Pb^{2+} concentration from 0 to 5×10^{-5} mol L^{-1}, indicating a change in the protein skeleton and its secondary structure (Wu et al., 2007). Fig. 6c–e show the UV–Vis spectra of the Phe residue, disulfide bond and tetrapyrrole of phycocyanin, respectively. No significant red-shift or blue-shift of

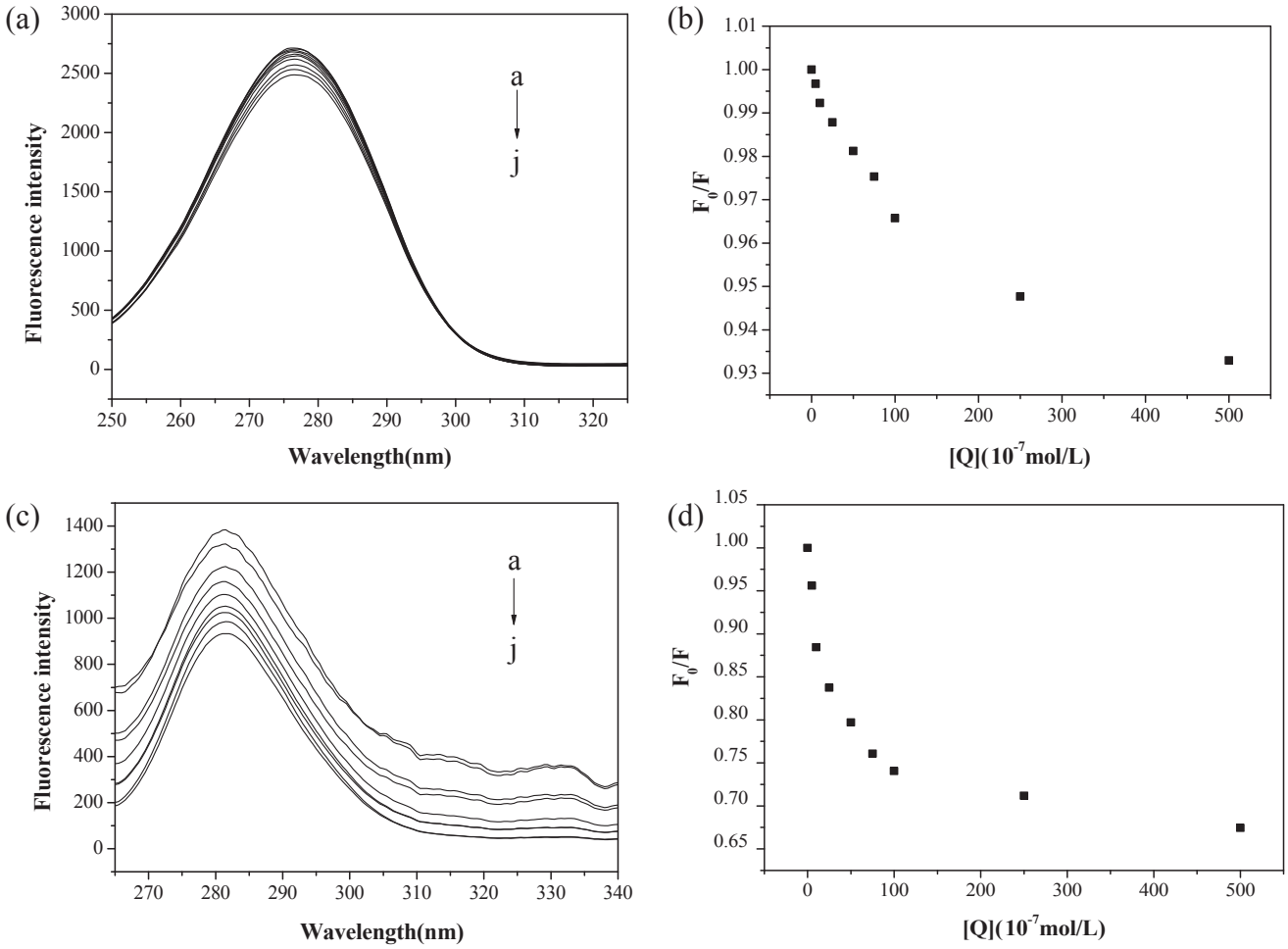

Fig. 4. Synchronous fluorescence spectra of phycocyanin samples with the Pb^{2+} concentrations of ($x10^{-6}$ mol L^{-1}) 0, 0.5, 1, 2.5, 5, 7.5, 10, 17.5, 25 and 50 (from sub-a to sub-j) at Δλ of 60 nm (a) or 15 nm (c); F_0/F plot for the synchronous fluorescence spectra of phycocyanin samples at Δλ of 60 nm (b) or 15 nm (d); λ_{ex} is 278 nm;; Concentration of phycocyanin is 5.0×10^{-7} mol L^{-1}; Temperature is 298 K; pH is 7.0.

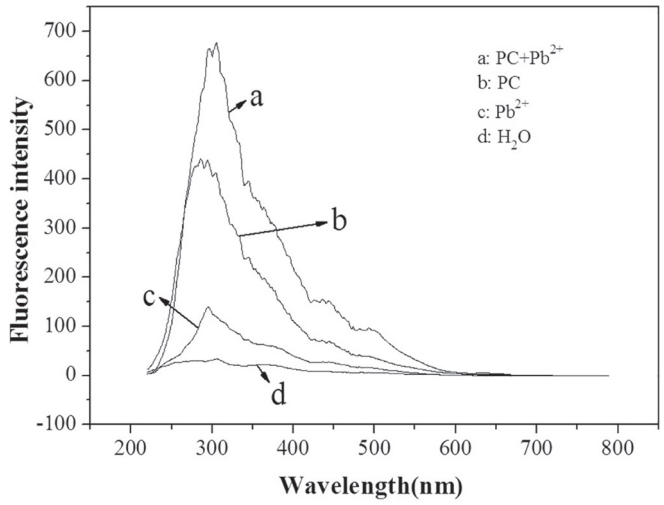

Fig. 5. Resonance light scattering spectra of phycocyanin-Pb^{2+} solution (a), phycocyanin solution (b), Pb^{2+} solution (c) and pure water (d) at 298 K; Concentration of phycocyanin is 5.0×10^{-7} mol L^{-1}; Concentration of Pb^{2+} is 5.0×10^{-6} mol L^{-1}; pH is 7.0.

the spectra is observed with increasing the Pb^{2+} concentration. Therefore the change in the protein skeleton and its secondary structure of phycocyanin is suggested to be a main reason to the fluorescence quenching by Pb^{2+}.

Fig. 7 show the circular dichroism spectra of phycocyanin samples with the Pb^{2+} concentrations of ($x10^{-6}$ mol L^{-1}) 0, 1, 2.5, 5 and 10 in the wavelength range of 190–260 nm (Fig. 7a) and 204–228 nm (Fig. 7b) for α-helix structure of protein (Lu et al., 2007). The negative peaks of α-helix structure locate at 209 nm and 218 nm. With the increasing Pb^{2+} concentration, the two negative peaks become smaller, showing a decrease content of the α-helix structure. The change in the secondary structure of phycocyanin protein may due to interactions between Pb^{2+} with the amino acid residues of phycocyanin skeleton, resulting in possible loss of functions of phycocyanin (Melo et al., 1997).

4. Conclusions

This work studied the influence of Pb^{2+} on fluorescence characteristics and protein structure of phycocyanin molecules experimentally *in vitro*. The fluorescence intensity decreased with increasing the concentration of Pb^{2+} from 0 to 5×10^{-5} mol L^{-1}, showing the fluorescence quenching of phycocyanin by Pb^{2+}. The quenching process was suggested to be static regarding the calculation results and the experimental results of time-resolved

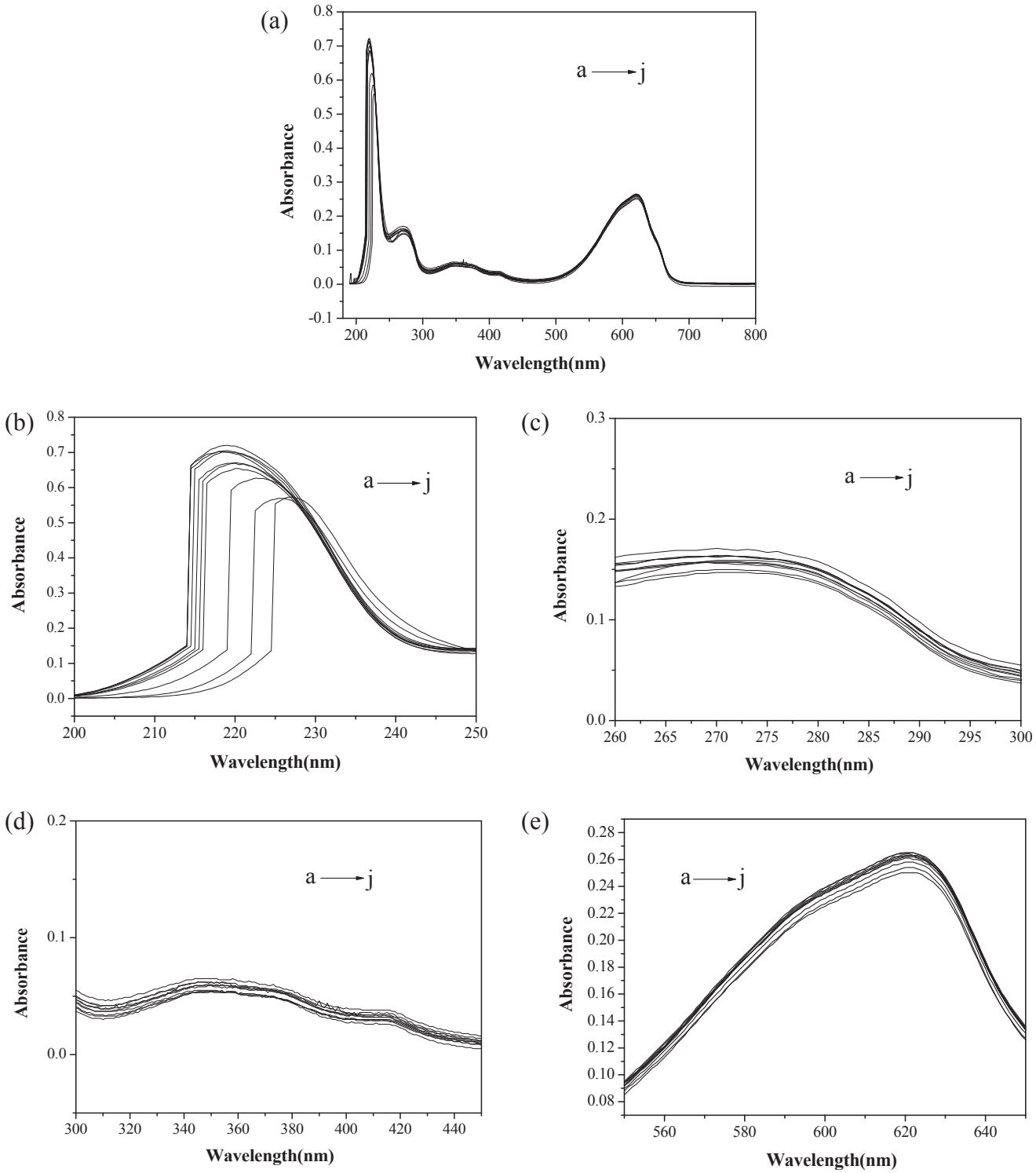

Fig. 6. UV–Vis spectra of phycocyanin samples with the Pb^{2+} concentrations of ($x10^{-6}$ mol L^{-1}) 0, 0.5, 1, 2.5, 5, 7.5, 10, 17.5, 25 and 50 (from sub-a to sub-j) in the wavelength range of 190–800 nm (a), 200–250 nm for protein skeleton (b), 260–300 nm for Phe residue (c), 300–450 nm for disulfide bond (d) and 550–650 nm for tetrapyrrole (vs the same concentration of Pb^{2+} solution); Concentration of phycocyanin is 5.0×10^{-7} mol L^{-1}; Temperature is 298 K; pH is 7.0.

fluorescence decay profiles. The synchronous fluorescence spectra showed that the effect of Pb^{2+} on the Tyr residues of phycocyanin was more significant than the Trp residues. The interaction of Pb^{2+} with phycocyanin molecules can result in the forming of aggregation analyzed by the resonance light scattering spectra. The UV–Vis spectra of the protein skeleton of phycocyanin had a red-shift of about 10 nm with increasing the Pb^{2+} concentration from 0 to 5×10^{-5} mol L^{-1}, indicating a change in the protein skeleton and its secondary structure. With increasing the Pb^{2+} concentration, the two negative peaks (209 nm and 218 nm) on circular dichroism spectra became smaller, showing a decrease of the α-helix structure.

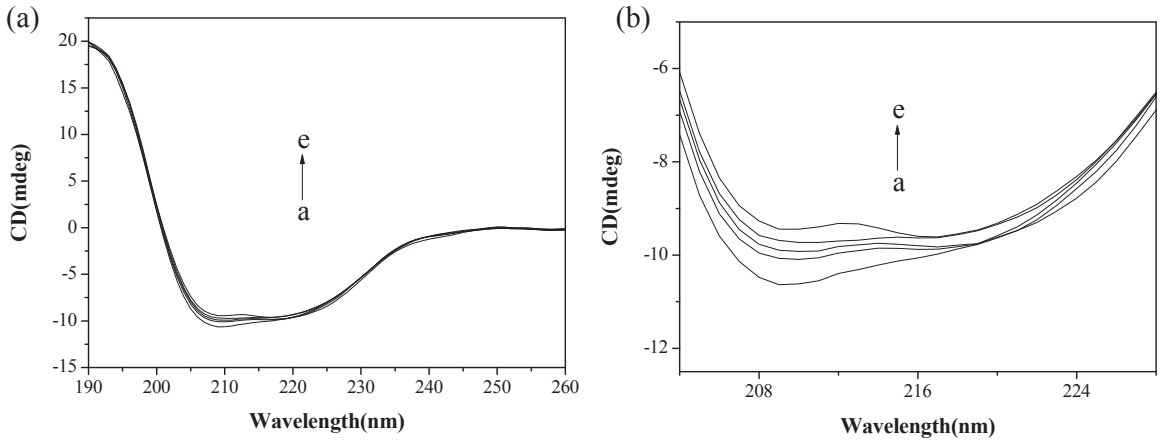

Fig. 7. Circular dichroism spectra of phycocyanin samples with the Pb^{2+} concentrations of ($x10^{-6}$ mol L^{-1}) 0, 1, 2.5, 5 and 10 (from sub-a to sub-e) in the wavelength range of 190–260 nm (a) and 204–228 nm for α-helix structure of protein (b); Concentration of phycocyanin is 5.0×10^{-7} mol L^{-1}; Temperature is 298 K; pH is 7.0.

Acknowledgements

This work was supported by the National Natural Science Foundation of China (21707026), the Guangzhou Key Laboratory of Environmental Exposure and Health (No. GZKLEEH201613), and the Shandong Provincial Natural Science Foundation, China (ZR2014BQ033). The Natural Scientific Research Innovation Foundation in Harbin Institute of Technology (HIT.NSRIF.2014126) is also acknowledged.

References

Aki, H., Yamamoto, M., 1989. Thermodynamics of the binding of phenothiazines to human plasma, human serum albumin and α1-acid glycoprotein: a calorimetric study. J. Pharm. Pharmacol. 41, 674–679.
Arunakumara, K., Zhang, X., 2009. Effects of heavy metals (Pb2+ and Cd2+) on the ultrastructure, growth and pigment contents of the unicellular cyanobacterium Synechocystis sp. PCC 6803. Chin. J. Oceanol. Limnol. 27, 383.
Arunakumara, K., Zhang, X., Song, X., 2008. Bioaccumulation of Pb2+ and its effects on growth, morphology and pigment contents of Spirulina (Arthrospira) platensis. J. Ocean Univ. China 7, 397–403.
Bhayani, K., Mitra, M., Ghosh, T., Mishra, S., 2016. C-Phycocyanin as a potential biosensor for heavy metals like Hg 2+ in aquatic systems. Rsc Adv. 6, 111599–111605.
Bobone, S., van de Weert, M., Stella, L., 2014. A reassessment of synchronous fluorescence in the separation of Trp and Tyr contributions in protein emission and in the determination of conformational changes. J. Mol. Struct. 1077, 68–76.
Burnett, M., Patterson, C., 2015. Analysis of Natural and Industrial Lead in Marine Ecosystems. Lead in the Marine Environment. In: Proceedings of the International Experts Discussion on Lead Occurrence, Fate and Pollution in the Marine Environment, vol. 18–22. Elsevier, Rovinj, Yugoslavia, p. 15. October 1977.
Chi, Z., Li, S., Wen, Z., Shan, Y., 2017. Mechanism of the toxicological interactions of decabrominated diphenyl ether with hemoglobin. Spectrosc. Lett. 50, 381–386.
Chi, Z., Zhao, J., You, H., Wang, M., 2016. Study on the interaction mechanism between phthalate acid esters and bovine hemoglobin. J. Agric. Food Chem. 64, 6035–6041.
do Sul, J.A.I., Costa, M.F., 2014. The present and future of microplastic pollution in the marine environment. Environ. Pollut. 185, 352–364.
Fu, Z., Cui, Y., Cui, F., Zhang, G., 2016. Modeling techniques and fluorescence imaging investigation of the interactions of an anthraquinone derivative with HSA and ctDNA. Spectrochim. Acta Part A Mol. Biomol. Spectrosc. 153, 572–579.
Geethanjali, H., Nagaraja, D., Melavanki, R., Kusanur, R., 2015. Fluorescence quenching of boronic acid derivatives by aniline in alcohols–A Negative deviation from Stern–Volmer equation. J. Luminescence 167, 216–221.
Gelagutashvili, E., 2007. Interaction of Heavy Metal Ions with C-phycocyanin: Binding Isotherms and Cooperative Effects. arXiv preprint arXiv:0707.3019.
Gu, W., Yan, Y., Pei, X., Zhang, C., Ding, C., Xian, Y., 2017. Fluorescent black phosphorus quantum dots as label-free sensing probes for evaluation of acetylcholinesterase activity. Sensors Actuators B Chem. 250, 601–607.
Jusoh, W.N.A.W., Wong, L.S., Chai, M.K., 2017. Phycocyanin Fluorescence in Whole Cyanobacterial Cells as Bioindicators for the Screening of Cu2+ and Pb2+ in Water.
Kannaujiya, V.K., Rahman, A., Sundaram, S., Sinha, R.P., 2016. Structural and functional dynamics of tyrosine amino acid in phycocyanin of hot-spring cyanobacteria: a possible pathway for internal energy transfer. Gene Rep. 5, 83–91.
Lu, J.-Q., Jin, F., Sun, T.-Q., Zhou, X.-W., 2007. Multi-spectroscopic study on interaction of bovine serum albumin with lomefloxacin–copper (II) complex. Int. J. Biol. Macromol. 40, 299–304.
Melo, E.P., Aires-Barros, M., Costa, S., Cabral, J., 1997. Thermal unfolding of proteins at high pH range studied by UV absorbance. J. Biochem. biophys. methods 34, 45–59.
More, A.F., Spaulding, N.E., Bohleber, P., Handley, M.J., Hoffmann, H., Korotkikh, E.V., Kurbatov, A.V., Loveluck, C.P., Sneed, S.B., McCormick, M., 2017. Next generation ice core technology reveals true minimum natural levels of lead (Pb) in the atmosphere: insights from the Black Death. GeoHealth 1, 211–219.
Pasternack, R.F., Collings, P.J., 1995. Resonance light scattering: a new technique for studying chromophore aggregation. Sci.-New York then Washingt. 269, 935–939.
Patel, A., Mishra, S., Pawar, R., Ghosh, P., 2005. Purification and characterization of C-phycocyanin from cyanobacterial species of marine and freshwater habitat. Protein Expr. Purif. 40, 248–255.
Peng, C., Zhao, X., Han, Y., Shi, W., Liu, S., Liu, G., 2015. Toxic effects of chronic sublethal Cu2+, Pb2+ and Cd2+ on Antioxidant enzyme activities in various tissuesof the blood cockle, anadara granosa. J. Residuals Sci. Technol. 12.
Rasoulzadeh, F., Asgari, D., Naseri, A., Rashidi, M.R., 2010. Spectroscopic studies on the interaction between erlotinib hydrochloride and bovine serum albumin. DARU J. Pharm. Sci. 18, 179.
Raspor, B., Nürnberg, H., Valenta, P., 2015. The Chelation of Lead by Organic Ligands in Sea Water. Lead in the Marine Environment. In: Proceedings of the International Experts Discussion on Lead Occurrence, Fate and Pollution in the Marine Environment, vol. 18–22. Elsevier, Rovinj, Yugoslavia, p. 181. October 1977.
Ross, P.D., Subramanian, S., 1981. Thermodynamics of protein association reactions: forces contributing to stability. Biochemistry 20, 3096–3102.
Saha, S., Mahato, P., Suresh, E., Chakrabarty, A., Baidya, M., Ghosh, S.K., Das, A., 2011. Recognition of Hg2+ and Cr3+ in physiological conditions by a rhodamine derivative and its application as a reagent for cell-imaging studies. Inorg. Chem. 51, 336–345.
Stoll, S., Gunn, A., Brynda, M., Sughrue, W., Kohler, A.C., Ozarowski, A., Fisher, A.J., Lagarias, J.C., Britt, R.D., 2009. Structure of the biliverdin radical intermediate in phycocyanobilin: ferredoxin oxidoreductase identified by high-field EPR and DFT. J. Am. Chem. Soc. 131, 1986–1995.
Tang, J.-X., Tang, Y.-Y., Sun, H.-X., Li, J.-R., WU, Y.A., 2013. Effects of Cu2+ and Pb2+(single factor and joint toxicity) on DNA damage in Misgurnus anguillicaudatus oocytes. Acta Hydrobiol. Sin. 37, 501–506.
Tao, S., Li, H., Liu, C., Lam, K., 2000. Fish uptake of inorganic and mucus complexes of lead. Ecotoxicol. Environ. Saf. 46, 174–180.
Wu, T., Wu, Q., Guan, S., Su, H., Cai, Z., 2007. Binding of the environmental pollutant naphthol to bovine serum albumin. Biomacromolecules 8, 1899–1906.
Zhang, X., Yang, L., Li, Y., Li, H., Wang, W., Ye, B., 2012. Impacts of lead/zinc mining and smelting on the environment and human health in China. Environ. Monit. Assess. 184, 2261–2273.